NOAA Technical Memorandum OAR PMEL-126

Background tides and sea level variations at Seaside, Oregon

Harold O. Mofjeld[1], Angie J. Venturato[2], Frank I. González[1], and Vasily V. Titov[2]

[1]Pacific Marine Environmental Laboratory
7600 Sand Point Way NE
Seattle, WA 98115-6349

[2]Joint Institute for the Study of the Atmosphere and Ocean (JISAO)
University of Washington
Box 354235
Seattle, WA 98195-4235

September 2004

Contribution 2736 from NOAA/Pacific Marine Environmental Laboratory

NOTICE

Mention of a commercial company or product does not constitute an endorsement by NOAA/OAR. Use of information from this publication concerning proprietary products or the tests of such products for publicity or advertising purposes is not authorized.

Contribution No. 2736 from NOAA/Pacific Marine Environmental Laboratory

For sale by the National Technical Information Service, 5285 Port Royal Road
Springfield, VA 22161

Contents

List of Figures

List of Tables

Background tides and sea level variations at Seaside, Oregon

Harold O. Mofjeld[1], Angie J. Venturato[2], Frank I. González[1], and Vasily V. Titov[2]

1. Introduction

The purpose of this technical memorandum is to provide a summary of the tides and other sea level variations at Seaside, Oregon, the site for the FEMA FIRM Tsunami Pilot Study. Because the tidal range is so large along the U.S. West Coast, the tides and other sea level variations have a significant effect on tsunami runup heights and inundation. For this reason, Houston and Garcia (1978) used predicted tides when computing the 100- and 500-year tsunami runup heights for the previous tsunami Flood Insurance Rate Maps (FIRMs).

Since Seaside is not served by a long-term tide station, many tidal quantities that are relevant to tsunami mapping must be estimated by other means. The results presented here are based on inferences from NOAA tide stations in the region and from the Eastern North Pacific ENPAC 2003 tide model of Spargo (2003) and Spargo *et al.* (in press). Tidal datums are available inside the mouth of the Necanicum River from water level observations taken during Nov 1971–Sept 1972; as we will see, there are substantial differences between these and the inferred coastal datums. The locations of the tide stations are shown in Fig. 1.

NOAA has designated the 19-year period 1983–2001 as the official U.S. National Tide Datum Epoch, and we have used observations from this NTDE when these were available. It is fortunate that the time series of water levels observed during this NTDE contain the largest El Niño events of the Twentieth Century (1982–1983 and 1997–1998), as well as representative distributions of other water level variations. This allows a useful comparison between observed and predicted tides in the region.

This technical memorandum is organized into examples of tidal time series to give a general characterization of the tides in the region (this section), tidal datums to provide information to develop digital elevation models and compare with tsunami amplitudes (Section 2), tidal harmonic constants that can be used for tidal prediction (Section 3), probability distributions including the average time the water level is at or above various heights (Section 4), interseismic sea level trends (Section 5), next steps to include background water levels in the estimation of 100- and 500-yr tsunami heights at Seaside area (Section 6), and conclusions on estimates of tides and other background water levels at Seaside (Section 7).

The examples of observed water levels in Fig. 2 show that within the central Cascadia region containing Seaside, the tides have very similar temporal patterns with some variation in amplitude between the tide stations.

[1]NOAA/Pacific Marine Environmental Laboratory, 7600 Sand Point Way NE, Seattle, WA 98115-6349

[2]Joint Institute for the Study of the Atmosphere and Ocean (JISAO), University of Washington, Box 354235, Seattle, WA 98195-4235

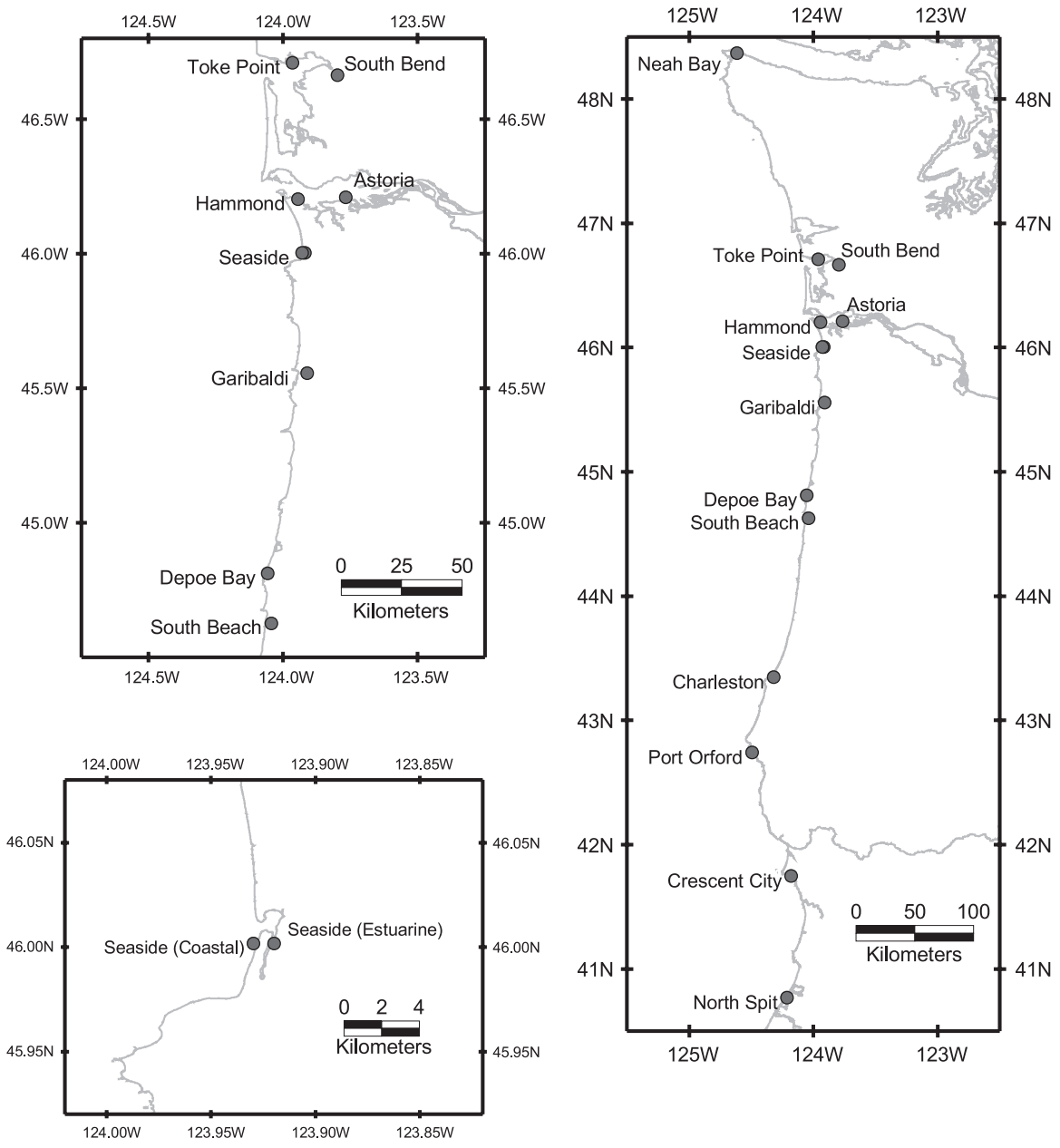

Figure 1: Map of the Central Cascadia region showing the locations of Seaside and relevant tide stations.

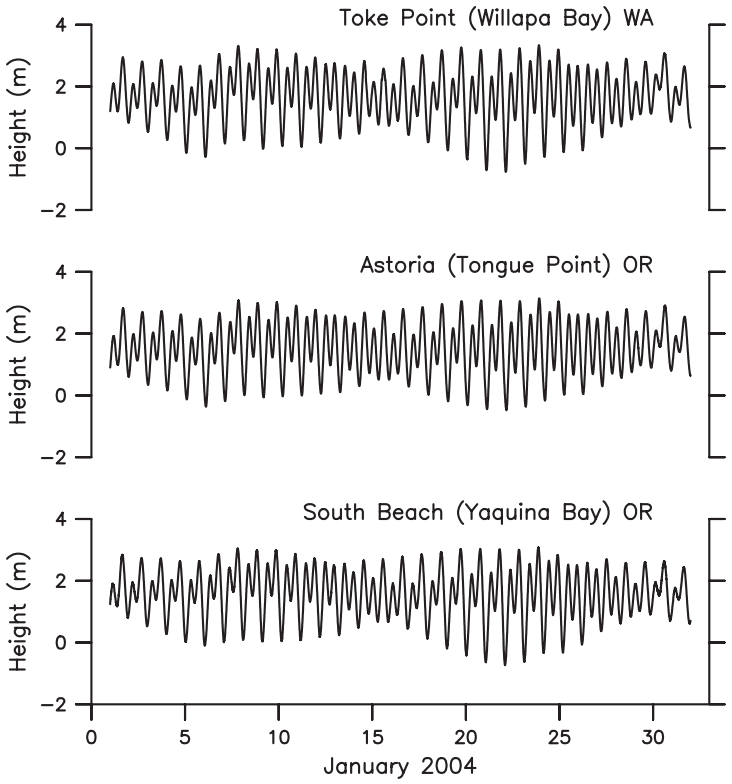

Figure 2: Sample time series of observed water levels at the three nearest long-term tide stations to Seaside.

These tides are mixed semidiurnal (Table 1). Substantial differences (Fig. 2) occur between successive low waters; lesser differences occur between successive high waters; and low and high waters follow the sequence LLW, LHW, HLW, HHW. Both the amplitude and shape of the daily tidal curve are modulated (Fig. 2) over fortnightly (two-week) and monthly time scales. The northward increase (Table 2) of the harmonic constant amplitudes and phase lags is consistent with northward propagating tidal waves that turn northwestward in the Cascadia region. Descriptions of the tidal modeling and dynamics in this region, as well as references to previous work, are given by Mofjeld *et al.* (1995), Foreman *et al.* (2000), Myers and Baptista (2001), Spargo (2003), and Spargo *et al.* (in press).

Observations and tidal theory show that the amplitudes and shapes of the daily tidal curve vary throughout the month due to variations in the lunar phase (new moon, first quarter...), declination (meridional angle off the equator), and parallax (distance from the earth). Significant modulations of the tides also occur on seasonal (solstitial-equinoctal and solar parallax) and interannual (18.6-year lunar nodal) time scales. For the latter reason, tidal datums (like those in the next section) are ideally computed from 19 years of observations (e.g., NTDE 1983–2001).

2. Tidal Datums

For the Tsunami Pilot Study, tidal datums are relevant in two ways. The first is in developing the digital elevation model (DEM) for the tsunami inundation model. The second is in providing a succinct summary of height scales for background water levels to compare with tsunami wave heights. Tidal datums are for the NTDE 1983–2001, computed from observations during this period or adjusted vertically to be consistent with it (details documented at NOAA's www.co-ops.nos.noaa.gov website).

Table 3 gives the official tidal datums for stations in the region surrounding Seaside as reported by NOAA/NOS/CO-OPS (National Ocean Service/Center for Operational Oceanographic Products and Services) and NOAA/NGS (National Geodetic Survey). For Seaside itself, three sets of datums are shown. The first set of coastal datums at Seaside were obtained by the harmonic constant datum method (Mofjeld *et al.*, 2004) using harmonic constants from the ENPAC 2003 tide model. The other set of coastal datums at Seaside were linearly interpolated in latitude from the observed datums at Hammond and Garibaldi (Fig. 1), the closest stations to Seaside. The third set of Seaside datums are based on 11 months (Nov 1971–Sept 1972) of water level observations at the 12th Avenue Bridge over the Necanicum River.

The coastal datums obtained by the two different methods are in relatively good agreement. For instance, the values of MHW relative to MLLW (important when merging water depth and land elevation data) agree within 0.2 m. However, there is a significant difference (Table 3) between the coastal datums and those inside the shallow river mouth. Of particular interest is the 0.76–0.96 m difference for MHW which is relevant to merging water depth and land elevation data to form the digital elevation model for tsunami modeling. It is worth noting that reduced tidal ranges often occur in bays with restrictive inlets (e.g., Kjerfve and Knoppers, 1991).

The larger difference (Table 3) between MLLW and the geodetic datum NAVD 88 observed inside the river mouth is also consistent with restricted tidal exchange through the inlet, especially near low tide when more water is retained in the estuary than would occur with free exchange. This hypothesis is corroborated by a personal communication from Maria Little (NOAA/NOS/CO-OPS) in which she reports that a water level station at the Seaside Sewage Plant (46° 0.4′N, 123° 55.1′W), just inside the river mouth, showed "...damping of the high waters and flat low waters, caused by a distortion of the tide signal. There are no Accepted Values [of tidal datums] for this station." The tidal exchange may additionally be affected by the changing nature of the river mouth as observed over the past 30 years. The variations in the river mouth will be discussed in a technical memorandum by Angie Venturato (in preparation). A high-resolution non-linear tide model would be needed to fully understand the relationship between the tides on the open coast at Seaside and those inside the Necanicum River mouth.

Table 1: Type of tide = (O1 + K1)/(M2 + S2) and sequence of tide = M2°−K1°−O1° at the nearest long-term tide stations to Seaside and inferred values for the open coast at Seaside. The Type of Tide is mixed semidiurnal when the amplitude ratio is between 0.25 and 1.5.

Station	**Type**	**Sequence (deg)**
Toke Point	0.563	127.2
Astoria	0.549	126.4
Coastal Seaside	0.611	130.7
South Beach	0.621	132.4

Table 2: M2 and K1 tidal harmonic constants observed at coastal and estuarine tide stations in the Cascadia region. These are the largest semidiurnal and diurnal constituents, respectively.

			M2		**K1**	
Station	**Latitude (deg)**	**Longitude (deg)**	**Amp H (m)**	**Lag G (deg)**	**Amp H (m)**	**Lag G (deg)**
Neah Bay	48.3683	124.6167	0.787	246.3	0.497	248.3
Toke Point	46.7083	123.9650	0.981	253.7	0.435	251.1
South Bend	46.6633	123.7983	1.124	259.7	0.428	254.8
Astoria	46.2083	123.7667	0.945	264.2	0.403	256.2
Coastal Seaside	46.0017	123.9300	0.960	229.1	0.463	238.2
Depoe Bay	44.8100	124.0583	0.890	225.0	0.438	235.0
South Beach	44.6250	124.0433	0.902	231.1	0.443	237.7
Charleston	43.3450	124.3217	0.818	225.3	0.401	235.2
Port Orford	42.7400	124.4967	0.750	216.5	0.428	231.2
Crescent City	41.7450	124.1833	0.714	212.2	0.390	228.2
North Spit	40.7667	124.2167	0.710	220.0	0.411	236.1

Table 3: Tidal datums relative to MLLW at tide stations in the region surrounding Seaside. The coastal Seaside datums were linearly interpolated in latitude using the datums at Hammond and Garibaldi. Also shown are the maximum and minimum observed heights at the tide station (where available) and the geodetic datums NGVD 29 and NAVD 88.

Station	**Hammond**	**Coastal Seaside**	**Coastal Seaside**	**Estuarine Seaside**	**Garibaldi**	**South Beach**
Source:	**Observed**	**Model**	**Interpolated**	**Observed***	**Observed**	**Observed**
Latitude	**46.2017**	**46.0017**	**46.0017**	**46.0017**	**45.5550**	**44.6250**
Longitude	**123.9450**	**123.9300**	**123.9300**	**123.9200**	**123.9117**	**123.0433**
To Entrance	**7 km**	**0 km**	**0 km**	**2 km**	**2 km**	**4 km**
	(m)	**(m)**	**(m)**	**(m)**	**(m)**	**(m)**
Max Obs	3.45				3.60	3.73
MHHW	2.54	2.74	2.52	1.77	2.48	2.54
MHW	2.33	2.51	2.31	1.55	2.26	2.33
MTL	1.36	1.47	1.35	0.84	1.35	1.38
MSL	1.34	1.46	1.34	0.83	1.33	1.36
MLW	0.39	0.44	0.39	0.12	0.40	0.42
NGVD29				0.23	1.16	1.26
NAVD 88	−0.01	−0.03 to 0.02		−0.88	0.10	0.23
MLLW	0.00	0.00	0.00	0.00	0.00	0.00
Min Obs	−0.90				−0.88	−1.07

*Maria Little, NOAA/NOS/CO-OPS, personal communication

3. Tidal Harmonic Constants

Tidal predictions rely on harmonic constants (HCs) that are specific to the location of interest. For the open coast at Seaside (46° 00.1′N, 123° 55.8′W), the HCs for the O1, K1, N2, M2, and S2 constituents were computed from the ENPAC 2003 tide model. The minor diurnal and semidiurnal HCs (Table 4) were inferred from South Beach amplitude ratios and phase differences using the method outlined by Schureman (1976). The long period HCs are based on those at South Beach. The higher frequency tides (2SM2, ...) are set to zero amplitude because of lack of information. However, they are likely to be small because the continental shelf west of Seaside is narrow and deepens relatively rapidly; this limits greatly the shallow water effects that generate such constituents. Also shown for comparison are observed HCs at Toke Point and South Beach (Fig. 1). The 37 constituents in Table 4 are the same as those used by NOAA for its official tidal predictions.

4. Water Level Probability Distributions

Probability distributions serve to characterize the general behavior of background water levels in terms of the duration of time spent at various ranges of height. To apply this method, the probability distribution functions (pdfs) are computed from observed tide gage records when these are available, or from predicted tides.

4.1 Observed Background Water Levels Near Seaside

Shown in Fig. 3 are the observed pdfs at Toke Point, Astoria, and South Beach (Fig. 1). The pdfs were computed by first interpolating the verified hourly observations to 15-minute values using cubic interpolation. The 15-minute time interval was chosen to allow accurate estimates for the heights of the individual high and low tides that may not be resolved with 1-hr sampling. The height values in the time series were binned using a 0.1 m height interval for each bin to form a histogram for each station. The histograms were then renormalized so that the total (sum) over the full range of heights is unity (1.0), as required by probability theory.

Figure 3 shows that the pdfs at the three stations tend to be large around the frequently occurring high and low water stands, when the height is changing slowly, but much smaller at the extreme ranges that occur only rarely in time. The pdfs at these stations are very similar. The slight upward displacement of the upper Toke Point and Astoria curves relative to the South Beach pdf is due to the slightly larger tidal ranges at these two stations. The shapes of the pdf curves are somewhat different near the central peaks (pdf > 0.3); but overall, the pdfs have very similar shapes and widths (Table 5) and similar maximum values. This is expected since the distances between the stations are small compared with the alongshore variations in tides in the Cascadia region (Mofjeld *et al.*, 1995; Foreman *et al.*, 2000; Myers and Baptista, 2001; Spargo, 2003; Spargo *et al.*, in press). The same should therefore be true on the open coast of Seaside since it is located between

Table 4: Tidal harmonic constants (37 constituents) and the mean relative to MLLW for the open coast at Seaside and at the Toke Point and South Beach tide stations.

Station:	**Toke Point**		**Coastal Seaside**		**South Beach**	
Location:	**46.7083, 123.9650**		**46.0017, 123.9300**		**44.6250, 124.0433**	
Constituent	**Amplitude H (m)**	**Phase Lag G (deg)**	**Amplitude H (m)**	**Phase Lag G (deg)**	**Amplitude H (m)**	**Phase Lag G (deg)**
mean	1.458		1.441		1.358	
SA	0.158	289.8	0.123	281.6	0.123	281.6
SSA	0.000	0.0	0.019	258.7	0.019	258.7
MM	0.000	0.0	0.027	174.7	0.027	174.7
MSF	0.000	0.0	0.000	0.0	0.000	0.0
MF	0.024	161.8	0.019	155.0	0.019	155.0
2Q1	0.006	221.0	0.007	202.2	0.007	204.3
Q1	0.047	230.2	0.050	216.7	0.048	213.4
RHO	0.011	208.7	0.011	212.4	0.010	213.8
O1	0.264	235.4	0.288	220.2	0.269	221.0
M1	0.016	270.3	0.016	252.2	0.015	250.7
P1	0.136	249.2	0.144	235.5	0.137	234.2
S1	0.006	40.7	0.012	20.4	0.012	20.4
K1	0.435	251.1	0.463	238.2	0.443	237.7
J1	0.023	267.6	0.029	256.8	0.027	255.0
OO1	0.016	292.6	0.016	276.4	0.015	273.1
2N2	0.022	204.6	0.022	178.2	0.021	183.2
MU2	0.008	253.2	0.016	197.2	0.015	201.1
N2	0.198	229.7	0.196	203.7	0.187	207.2
NU2	0.044	228.6	0.038	206.1	0.036	209.5
M2	0.981	253.7	0.960	229.1	0.902	231.1
LAM2	0.009	269.3	0.006	241.2	0.006	243.8
L2	0.033	266.3	0.026	243.6	0.024	246.4
T2	0.017	270.5	0.015	250.6	0.014	253.8
S2	0.261	284.4	0.269	255.2	0.244	258.6
R2	0.002	285.6	0.002	255.2	0.002	258.6
K2	0.071	279.6	0.070	247.4	0.066	250.2
2SM2	0.000	0.0	0.000	0.0	0.003	63.5
2MK3	0.005	64.3	0.000	0.0	0.000	0.0
M3	0.000	0.0	0.000	0.0	0.000	0.0
MK3	0.004	10.9	0.000	0.0	0.004	172.3
MN4	0.006	335.6	0.000	0.0	0.005	164.8
M4	0.014	352.6	0.000	0.0	0.013	189.0
MS4	0.009	30.5	0.000	0.0	0.007	229.5
S4	0.000	0.0	0.000	0.0	0.000	0.0
M6	0.009	45.3	0.000	0.0	0.008	300.7
S6	0.000	0.0	0.000	0.0	0.000	0.0
M8	0.000	0.0	0.000	0.0	0.000	0.0

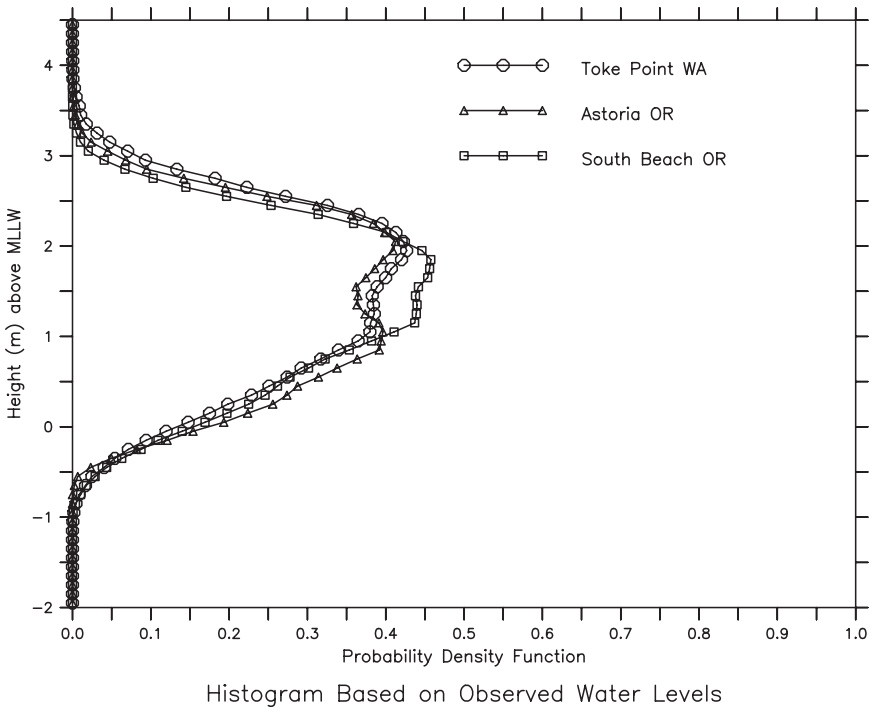

Figure 3: Probability density functions computed from observed water levels at the nearest long-term tide stations to Seaside.

these tide gage stations. Other differences in the pdfs are presumably due in part to local tidal dynamics within the three bays where the tide gages are located and to different inlet effects on the tides in these bays.

Integrating the pdfs (Fig. 3) downward in height gives the cumulative exceedance probability P(η), where η is the height above MLLW. P(η) represents the fraction of the time, on average, that the water level is above the height η. As shown in Fig. 4, the exceedance probabilities decrease approximately linearly with increasing height η from MLLW ($\eta = 0$) to P = 0.1 (10% probability of exceedance). The differences in P between the three tide stations increases upward in height to a 0.19 m difference between Toke Point and South Beach at P = 0.1.

The values of P at larger heights are relevant to the exceedance probabilities of observed storm surges. When plotted on a log(P) scale, the exceedance curves (Fig. 5) take an asymptotic form that can be fit to extreme value distributions. Like the tsunami probability distributions, additional calculations using time series of storm surges, especially their duration in time, need to be performed before distributions like those in Fig. 5 can be used to determine event heights for various recurrence intervals (Pugh, 1987, 2004).

The percentage heights and ranges shown in Table 5, as well as the magnitudes of the tidal datums given in Table 3, indicate that tides are large enough to have important effects on the height probabilities of tsunamis at Seaside. The percentage height ranges (Table 5) for the three stations are

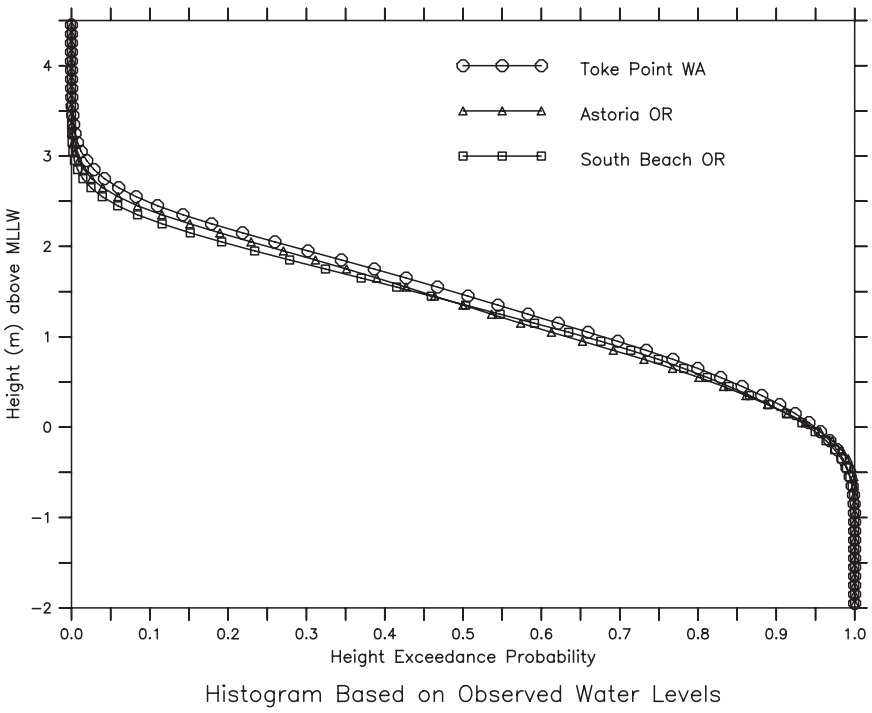

Figure 4: Exceedance probabilities computed from observed hourly water levels at the nearest long-term tide stations to Seaside.

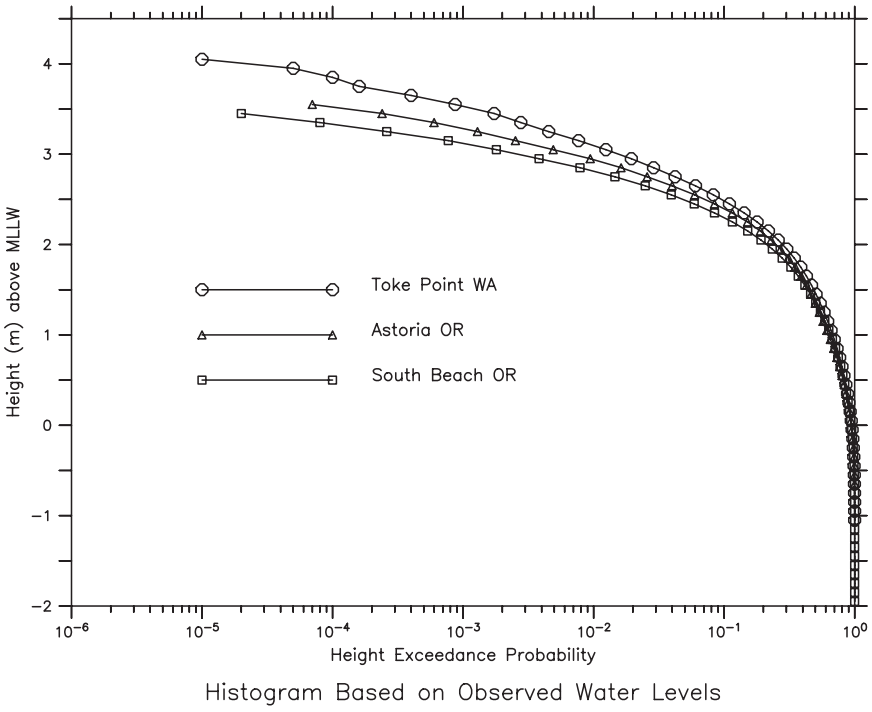

Figure 5: Same as Fig. 4 but with the logarithm of exceedance probability plotted against height.

Table 5: Percentage heights and ranges, based on the probability distribution functions derived from observed water levels during the National Tidal Datum Epoch 1983–2001. For a given percentage probability, a random background water level will occur within the height range between the upper and lower bounds.

Station		**Height Ranges**			
Bounds (%):	**50% Height (m)**	**50% (m)**	**80% (m)**	**90% (m)**	**98% (m)**
Toke Point	1.47				
Upper		2.00	2.30	2.50	2.82
Lower		0.70	0.21	−0.05	−0.46
Range		1.30	2.09	2.55	3.28
Astoria	1.35				
Upper		2.00	2.40	2.60	2.94
Lower		0.70	0.21	−0.02	−0.33
Range		1.30	2.19	2.62	3.27
South Beach	1.36				
Upper		2.07	2.49	2.71	3.10
Lower		0.80	0.27	−0.01	−0.45
Range		1.27	2.22	2.72	3.55

very similar, differing by less than 0.2 m for probabilities of 90% or less. Hence, these statistics are spatially uniform within a few tenths of a meter at Toke Point, Astoria, and South Beach. By implication, the same is true along the open coast at Seaside.

4.2 Predicted Background Water Levels at Seaside

Houston and Garcia (1978) used predicted tides to compute the effects of background water level fluctuations on the 100- and 500-year tsunami exceedance heights along the West Coast. Since observed water levels are available at only a limited number of sites along the West Coast and these are typically within embayments, there is an issue as to whether predicted tides can be used for the next generation of tsunami flood maps.

As a measure of the differences between the observed and predicted water levels that might occur at Seaside, a comparison between these was made for the water levels at South Beach. These are then compared with the predicted tides at Seaside. The pdf and exceedance probabilities were computed from 19-year (NTDE 1983–2001) time series of hourly tidal predictions (cubic interpolated to 15-minute values to be consistent with the procedures used on the observed time series). The South Beach and Seaside harmonic constants used to generate the predictions are shown in Table 4. The height exceedance probabilities in Figs. 6 and 7 provide a measure of how much error would occur on average by using predicted rather than observed water levels for Seaside, since both South Beach and Seaside are located within the same meteorological and oceanographic regimes. The differences in the Seaside curves relative to those for South Beach are primarily due to the larger tidal range at Seaside, as seen in Figs. 3 and 5 for Astoria and Toke Point.

From the standpoint of probabilities (Figs. 6 and 7), there is very close

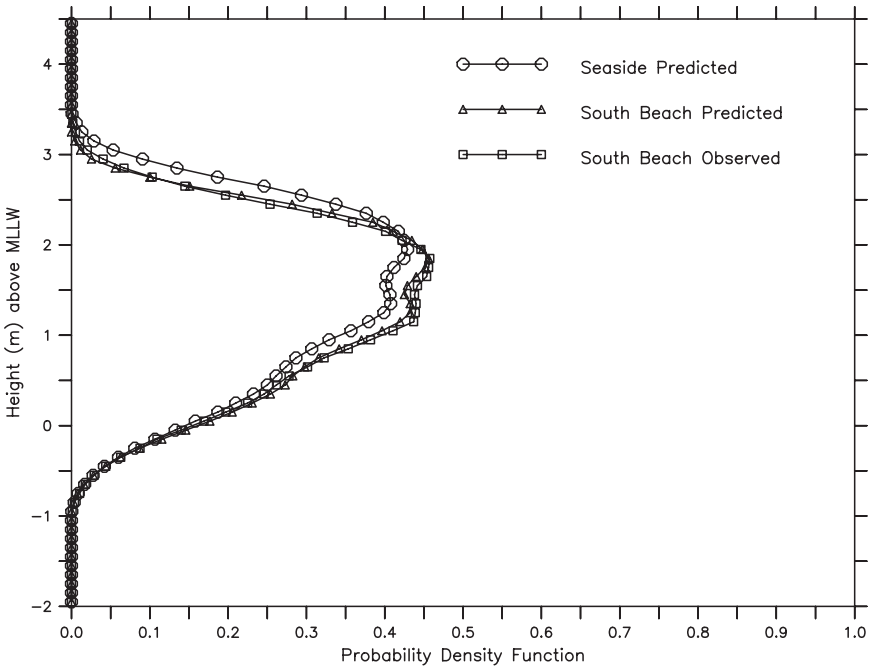

Figure 6: Probability density functions (pdfs) computed from predicted water levels at South Beach and Seaside. Also shown is the pdf computed from the observed water levels at South Beach.

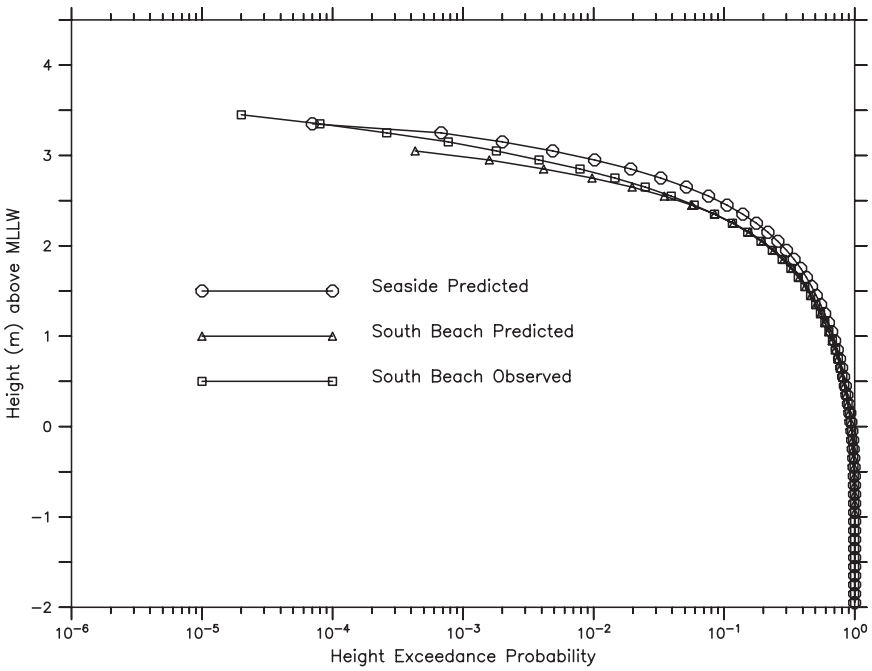

Figure 7: Same as Fig. 6 but with the logarithm of exceedance probability plotted against height.

agreement between the observations and predictions for South Beach. The minor differences that do exist (Figs. 6 and 7) are due primarily to the storm surges and other non-tidal water level fluctuations that are not included in the tidal predictions. These give rise to the greater heights at low exceedance probabilities (Fig. 7). However, there is a very low probability that the maximum wave in a tsunami will arrive at Seaside at the same time as a winter storm, occurring during a major El Niño, than at lower heights where there is a very close match between the observed and predicted tides.

5. Sea Level Trends

When presenting the broad spectrum of coastal water levels, it is appropriate to also include a discussion of sea level trends. This is true even though they are not immediately relevant to the specific issues of computing 1-percentage-annual-chance and 0.2-percentage-annual-chance quantities that are FEMA's definitions for the 100- and 500-yr exceedance values, respectively.

The sea level trends (Table 6) in the Cascadia region vary considerably between long-term tide stations. This indicates different vertical ground movement in the vicinity of the tide gages that are significant in magnitude compared with the present ∼1.4 mm/yr of global sea level rise (Intergovernmental Panel on Climate Change (IPCC), 2001; Pugh, 2004). The upward ground movement at Neah Bay and Crescent City (Fig. 1) is large enough to overwhelm oceanic sea level rise and produce negative trends that are significant at the 95% confidence level. In contrast, the observed trend at South Beach indicates continuing subsidence of the land near the tide gage.

The variation in trends (Table 6) along the length of Cascadia shows that the interseismic tectonic processes presently affecting relative sea level also vary with location along the coast. Given this variability, it is difficult to estimate the sea level trend at Seaside based solely on the observed trends elsewhere in the region. The observed trends at other sites serve as placing some bounds of the Seaside trend and, taken together with other information from GPS observations and geological interpretation, may help to further constrain estimates of the interseismic Seaside trend. There is also the important issue of coseismic ground movement (subsidence or uplift) during regional Cascadia Subduction Zone earthquakes.

6. Joint Probability Methods Versus Direct Calculations

One method for including tides and other water level fluctuations in the probability estimates of coastal flooding is via the joint probability method (JPM) described by, e.g., Tawn and Vassie (1991) and Pugh (1987, 2004). This method convolves (integrates their product over height) the pdf of the background water levels at a given coastal location with the pdf of modeled storm surges to get the total exceedance probability. The revised method (Tawn and Vassie, 1991) adjusts the probabilities to take into account the

Table 6: Observed sea level trends at tide stations in the Cascadia region. Shown are trends in relative sea level, which are the sum of the separate vertical movements of the water and the land. Note that the uncertainty in the trend decreases with increasing series length.

Station	Trend (mm/yr)	Stnd. Dev. (mm/yr)	95% C I (mm/yr)	Start	End	Length (years)
Neah Bay	−1.41	0.22	0.43	1934	1999	66
Toke Point	2.82	1.05	2.06	1973	1999	27
Astoria	−0.16	0.24	0.47	1925	1999	75
South Beach	3.51	0.73	1.43	1967	1999	33
Charleston	1.74	0.87	1.71	1970	1999	30
Crescent City	−0.48	0.23	0.45	1933	1999	67

non-random nature of the tides and the persistence in time (redundancy) of both the tides and the additional flooding event (e.g., storm surge), as well as possible non-linear interactions between tsunamis and the tides. A major issue in applying the revised JPM method to the tsunami problem would be finding the redundancy factors for the model tsunamis and background water levels.

An alternative to this method is that of Houston and Garcia (1978), in which each model tsunami is slid along the time series of background water levels. Since the time series of the model tsunamis are relatively short compared to the duration of significant waves in observed tsunamis, the model time series need to be extended in time. This can be done by assuming exponential amplitude decay, which Mofjeld *et al.* (2000) have shown matches closely the observed decay of Pacific tsunamis.

7. Summary and Conclusions

For tides on the open coast at Seaside, Oregon, a comparison has been made of predictions based on the ENPAC 2003 tide model of Spargo (2003) and Spargo *et al.* (in press) with the observed and predicted water levels at long-term tide stations in the region. This comparison shows there is close agreement for many of the tidal quantities that are relevant to probabilistic tsunami mapping. This is fortunate, since Seaside is not served by a long-term tide station. The tidal datums inferred from the model harmonic constants and those interpolated from observed values at Hammond and Garibaldi (Fig. 1) are found to be within 0.05 m for MHW relative to MLLW. Having an accurate estimate of this height difference is essential for generating the digital elevation model (DEM) for tsunami modeling. There are substantial differences between the coastal datums at Seaside and those observed within the Necanicum River, possibly due to restricted tidal exchange through the river mouth.

Close agreement exists between probability distributions at the long-term South Beach station and those at the Seaside open coast. This is due in part to the proximity of the South Beach station to the coast and the free tidal exchange through the inlet to Yaquina Bay. Conversely, the comparison

of tidal quantities at Toke Point, Astoria, and South Beach (Fig. 1) reveals greater differences, probably at least partly due to local tidal dynamics in the bays where these tide stations are located. However, the exceedance curves from all the tide stations are very close to each other and, by implication, to that on the outer coast at Seaside. These results also suggest that predicted tides should be adequate when linearly combining coastal tsunami heights with background water levels to estimate probabilities.

The goal of the Tsunami Pilot Study is to develop methods that can be applied to probabilistic tsunami hazard assessment and mapping along the U.S. West Coast. The analyses and comparison outlined in this technical memorandum, together with the distribution of long-term tide stations along the Coast, suggest that the methods used here will work effectively to characterize background water levels at other locations where direct long-term water level observations are not available.

8. Acknowledgments

The authors wish to thank Maria Little (NOAA/NOS/Center for Operational Oceanographic Products and Services), Emily Spargo, Ed Myers (NOAA/NOS/Coastal Survey Development Laboratory), and Mike Foreman (Fisheries and Oceans Canada/Institute of Ocean Sciences) for providing datums, harmonic constants, and other useful tidal information.

References

Foreman, M.G.G., W.R. Crawford, J.Y. Cherniawsky, R.F. Henry, and M.R. Tarbotton (2000): A high-resolution assimilating tidal model for the northeast Pacific Ocean. *J. Geophys. Res.*, *105*(C12), 28,629–28,651.

Houston, J.R., and A.W. Garcia (1978): Type 16 Flood Insurance Study: Tsunami predictions for the West Coast of the Continental United States. USACE USACE Waterways Experimental Station Tech. Rprt H-78-26.

Intergovernmental Panel on Climate Change (IPCC) (2001): *Climate Change 2001: Impacts, Adaptation and Vulnerability*. Cambridge Univ. Press, 1032 pp.

Kjerfve, B., and B.A. Knoppers (1991): Tidal choking in a coastal lagoon. In *Tidal Hydrodynamics*, B.B. Parker (ed.), Wiley, 169–181.

Mofjeld, H.O., F.I. González, E.N. Bernard, and J.C. Newman (2000): Forecasting the heights of later waves in Pacific-wide tsunamis. *Nat. Hazards*, *22*, 71–89.

Mofjeld, H.O., F.I. González, M.C. Eble, and J.C. Newman (1995): Ocean tides in the continental margin off the Pacific Northwest Shelf. *J. Geophys. Res.*, *100*(C6), 10,789–10,800.

Mofjeld, H.O., A.J. Venturato, F.I. González, V.V. Titov, and J.C. Newman (2004): The harmonic constant datum method: Options for overcoming datum discontinuities at mixed-diurnal tidal transitions. *J. Atmos. Oceanic Tech.*, *21*, 95–104.

Myers, E.P., and A.M. Baptista (2001): Inversion for tides in the Eastern North Pacific Ocean. *Adv. Water. Resour.*, *24*(5), 505–519.

Pugh, D.T. (1987): *Tides, Surges and Mean Sea-Level*. Wiley, 472 pp.

Pugh, D.T. (2004): *Changing Sea Levels: Effects of Tides, Weather and Climate*. Cambridge Univ. Press, 265 pp.

Schureman, P. (1976): Manual of Harmonic Analysis and Prediction of Tides. C&GS Spec. Publ. No. 98, U.S. Government Printing Office, 317 pp.

Spargo, E., J. Westerink, R. Luettich, and D. Mark (2004): Developing a tidal constituent database for the Eastern North Pacific Ocean. In *Proceedings of the 8th International Conference on Estuarine and Coastal Modeling*, Monterey, CA, 3–5 November 2003, in press.

Spargo, E.A. (2003): Using a Finite Element Model of the Shallow Water Equations to Model Tides in the Eastern North Pacific Ocean. M.S. Thesis, University of Notre Dame, 224 pp.

Tawn, J.A., and J.M. Vassie (1991): Recent improvements in the joint probability method for estimating extreme sea levels. In *Tidal Hydrodynamics*, B.B. Parker (ed.), Wiley, 813–828.

Venturato, A.J. (in preparation): A digital elevation model for Seaside, Oregon: Procedures, data sources, and analyses. NOAA Tech. Memo.